Spectrochimica Acta Part A: Molecular and Biomolecular Spectroscopy 98 (2012) 35–42

Contents lists available at SciVerse ScienceDirect

Spectrochimica Acta Part A: Molecular and Biomolecular Spectroscopy

journal homepage: www.elsevier.com/locate/saa

Synthesis and characterization of VO(II), Co(II), Ni(II), Cu(II) and Zn(II) complexes of chromone based azo-linked Schiff base ligand

C. Anitha [a], C.D. Sheela [b], P. Tharmaraj [a,*], S. Johnson Raja [c]

[a] Department of Chemistry, Thiagarajar College, Madurai 625 009, India
[b] Department of Chemistry, The American College, Madurai 625 002, India
[c] Department of Chemistry, Raja College of Engineering and Technology, Madurai 625 020, India

HIGHLIGHTS

- Co-ordinating possibility of *p*-phenylenediamine has been proved by condensing with carbonyl compounds.
- All the complexes posses' octahedral geometry except oxovanadium complex which posses square pyramidal geometry.
- The Cu(II) and Zn(II) complexes show greater antibacterial activity.
- The azo ligand exert second-harmonic generation (SHG) efficiency.
- The synthesized compounds can be better accommodated for optical applications.

GRAPHICAL ABSTRACT

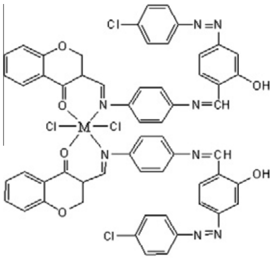

M = Co, Ni, Cu and Zn

ARTICLE INFO

Article history:
Received 7 March 2012
Received in revised form 12 July 2012
Accepted 12 August 2012
Available online 23 August 2012

Keywords:
Salicylaldehyde
Schiff-base complexes
Antimicrobial activity
Spectroscopy

ABSTRACT

Azo-Schiff-base complexes of VO(II), Co(II), Ni(II), Cu(II) and Zn(II) have been synthesized and characterized by elemental analysis, IR, UV–Vis, ^{1}H NMR, mass spectra, molar conductance, magnetic susceptibility measurement, electron spin resonance (EPR), CV, fluorescence, NLO and SEM. The conductance data indicate the nonelectrolytic nature of the complexes, except VO(II) complex which is electrolytic in nature. On the basis of electronic spectra and magnetic susceptibility octahedral geometry has been proposed for the complexes. The EPR spectra of copper and oxovanadium complexes in DMSO at 300 and 77 K were recorded and its salient features are reported. The redox behavior of the copper(II) complex was studied using cyclic voltammetry. The *in vitro* antimicrobial activity against *Staphylococcus aureus, Escherichia coli, Salmonella enterica typhi, Bacillus subtilis* and *Candida* strains was studied and compared with that of free ligand by well-diffusion technique. The azo Schiff base exhibited fluorescence properties originating from intraligand (π–π^*) transitions and metal-mediated enhancement is observed on complexation and so the synthesized complexes can serve as potential photoactive materials as indicated from their characteristic fluorescence properties. On the basis of the optimized structures, the second-order nonlinear optical properties (NLO) are calculated by using second-harmonic generation (SHG) and also the surface morphology of the complexes was studied by SEM.

Introduction

Schiff bases are most widely used as chelating ligands in coordination chemistry [1]. They are also useful in catalysis and in

---

* Corresponding author. Tel.: +91 9442555836; fax: +91 452 2311875.
E-mail address: rajtc1962@gmail.com (P. Tharmaraj).

1386-1425/$ - see front matter © 2012 Elsevier B.V. All rights reserved.
http://dx.doi.org/10.1016/j.saa.2012.08.022

medicine as antibiotics, antiallergic and antitumor agents [2]. Azo Schiff base ligands and their metal complexes have been extensively studied over past few decades. Of the various classes of Schiff base which can be prepared by condensation of different types of amines and carbonyl compounds, Schiff bases derived from chromone compounds have been the center of attraction for many workers in recent years. The chromone moiety forms the important component of the pharmacophores of a number of biologically active molecules of synthetic as well as natural origin and many of them have useful medicinal applications [3]. 3-Formyl chromone occupy a unique position for two reasons. They are carrying a significant biological activity and they are attractive synthetic intermediates [4]. The remarkable biological properties [5–9], proton affinities [10], optical properties and the degree of aromaticity [11] of the chromones have attracted considerable attention from both experimental and theoretical point of views. The 3-formylchromones have many applications. They are used as versatile synthons in heterocyclic chemistry [12–14]. In the pharmaceutical area, the potency and selectivity of derivates of 3-formylchromones, provides a novel pharmacophore for the design of drugs for the treatment of type II diabetes and obesity [15]. Earlier work has shown that some drugs showed increased activity when administered as metal chelates rather than as organic compounds and that the coordinating possibility of *p*-phenylenediamine has been improved by condensing with a variety of carbonyl compounds.

The present study aimed to investigate the Schiff base derived from the condensation of 5-(4-chloro-phenylazo)-2-hydroxy benzaldehyde, 3-formylchromone and p-phenylenediamine. The complexes of VO(II), Co(II), Ni(II), Cu(II) and Zn(II) were also prepared in the solid state and characterized by different physico-chemical methods.

Experimental

The chemicals and solvents were purchased from Aldrich Chemical & Co. and the common solvents used at various stages of this work are purified according to the standard procedures described in Weissenburg series [16]. Elemental analyses were carried out using a Perkin-Elmer 2400 II elemental analyzer. Molar conductance of the complexes was measured in DMSO at room temperature using a Systronic Conductivity Bridge 304. Magnetic susceptibility of the complexes was performed on a Sherwood MSB mark1 Gouy balance. Infrared spectral studies were carried out on a Shimadzu FT IR 8000 spectrophotometer using KBr discs. UV–Vis spectra were obtained using a THERMO SPECTRONIC 6 HEXIOS α and fluorescence spectra were determined with an ELICO SL174 spectrofluorometer. NMR spectra were recorded on Bruker DRX-300, 300 MHz NMR spectrometer using TMS as reference. EPR spectra of the Cu(II) and VO(II) complex was recorded in Varian E-112 machine at 300 and 77 K using TCNE (Tetracyanoethylene) as the g-marker. Cyclic voltammetric measurement for Cu(II) complex in DMSO was carried out on a Electrochemical analyzer CH Instruments (USA) using a three electrode cell containing an Ag/AgCl reference electrode, Pt wire auxiliary electrode and glassy carbon working electrode with tetrabutylammonium perchlorate as supporting electrolyte. Electron-ionization (EI) mass spectra were recorded by JEOL-GC Mass Spectrometer MATE-2. The second-harmonic generation (SHG) conversion efficiency of the Schiff base ligand was determined by the modified version of powder technique in IISc, Bangalore. SEM images were recorded in a Hitachi SEM analyzer.

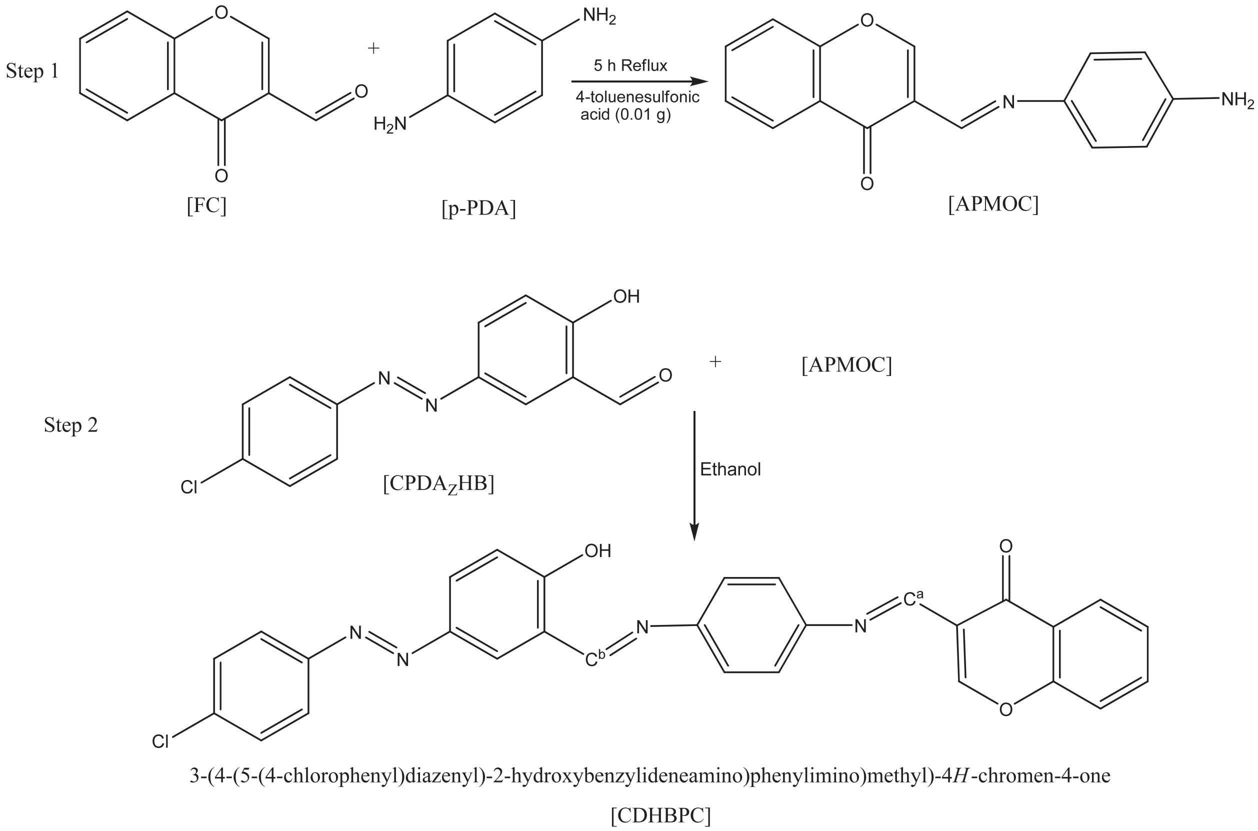

Fig. 1. Synthesis of azo Schiff base ligand.

Table 1
Physical characterization, analytical and molar conductance data of the ligand (CDHBPC) and its metal(II) complexes.

Compound	Analysis found (Calcd) (%)							
	Formula weight	M	C	H	N	Yield (%)	m.p. (°C)	Λ_M/S (cm^2 mol^{-1})
CDHBPC [$C_{29}H_{21}ClN_4O_3$]	506.11	–	68.70 (68.71)	3.75 (3.78)	11.02 (11.05)	75	297	–
[VOL_2]SO_4 [$C_{58}H_{42}Cl_2N_8O_{11}SV$]	1175.12	4.31 (4.33)	59.20 (59.19)	3.26 (3.25)	9.57 (9.52)	70	>360	56.8
[CoL_2Cl_2] [$C_{58}H_{42}Cl_4N_8O_6Co$]	1141.10	5.12 (5.15)	60.90 (60.91)	3.38 (3.35)	9.79 (9.80)	79	>360	10.7
[NiL_2Cl_2] [$C_{58}H_{42}Cl_4N_8O_6Ni$]	1140.10	5.12 (5.13)	60.95 (60.92)	3.37 (3.35)	9.79 (9.80)	68	>360	11.0
[CuL_2Cl_2 [$C_{58}H_{42}Cl_4N_8O_6Cu$]	1145.10	5.52 (5.53)	60.62 (60.66)	3.31 (3.34)	9.75 (9.76)	84	>360	10.4
ZnL_2Cl_2 [$C_{58}H_{42}Cl_4N_8O_6Zn$]	1146.10	5.67 (5.69)	60.58 (60.57)	3.31 (3.33)	9.77 (9.74)	82	>360	10.2

Synthesis of the ligand (CDHBPC)

3-Formylchromone (4-oxo-4H-chromene-3-carboxaldehyde) was prepared by the Vilsmeier–Haack synthesis [17]. A mixture of 4-oxo-4H-chromene-3-carboxaldehyde (0.87 g, 5 mmol) and 1,4-phenylenediamine (0.54 g, 5 mmol) in dry benzene (50 ml) containing 4-toluenesulfonic acid (0.01 g) was refluxed for 5 h. The obtained solid was filtered off and crystallized to give 3-[(4-Aminophenylimino)methyl]-4-oxo-4H-chromene [A]. Yield 78%, m.p. 201 °C. Schiff base ligand 3-(4-5-(4-chlorophenyl)diazenyl)-2-hydroxybenzylideneamino)phenylimino)methyl)-4H-chromen-4-one [CDHBPC] was prepared by refluxing the precursor ligand 3-[(4-Aminophenylimino)methyl]-4-oxo-4H-chromene(1.32 g, 5 mmol) [A] with 5-(4-Chloro-phenylazo)-2-hydroxy-benzaldehyde (1.3 g, 5 mmol) [18] for 5 h in ethanol medium. The red orange color solid obtained was separated out and recrystallized. Yield 70%. m.p. 297 °C (Fig 1).

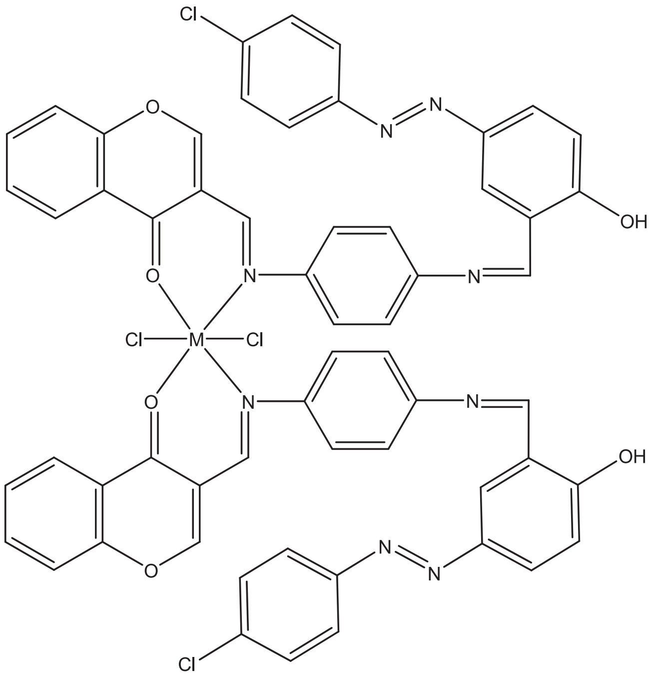

M = Co(II), Ni(II), Cu(II) and Zn(II)

Fig. 2. Proposed structure of metal(II) complexes.

Synthesis of complexes

A mixture of 2 mmol of ligand in ethanol was reacted with aqueous solution of metal chlorides/sulfates [$VOSO_4 \cdot 2H_2O$, $CoCl_2 \cdot 6H_2O$, $NiCl_2 \cdot 6H_2O$, $CuCl_2 \cdot 2H_2O$ and $ZnCl_2$]. (1 mmol). The reaction mixture was adjusted to pH 7–8 by adding NaOH and was stirred for 2 h at 40 °C. The solid obtained was collected, filtered, washed with ether, recrystallized from ethanol and dried under vacuum. The oxovanadium complex was synthesized from the ligand and oxovanadium sulfate by adopting the above method under reflux for 2 h at 40 °C and concentrating the solution through rotavaporation. The yield obtained was 65–70%.

Non linear optical (NLO) properties of the ligand

The SHG efficiency of the Schiff base was determined by modified version of powder technique developed by Kurtz and Perry [19]. The compound was ground into powder and packed between two transparent glass slides. A source of Nd:YAG laser beam of wavelength 1064 nm was made to fall normally on the sample cell. The second-harmonics signal, generated in the compound was confirmed from the emission of green radiation by the crystal. The SHG radiation of 532 nm green light was collected by a photomultiplier tube (PMT-Philips Photonics-model 8563) after being monochromated (monochromator-model Triax-550) to collect only the 532 nm radiation. The efficiency of the sample was compared with microcrystalline powder of KDP and urea. The input energy used in this particular setup was 2.2 mJ/pulse.

Biological activity

Antimicrobial activity of the compounds was tested *in vitro* by the well diffusion method [20] against the bacteria *Staphylococcus aureus, Escherichia coli, Salmonella enterica typhi, Bacillus subtilis* using agar nutrient as the medium. Also the antifungal activity against the fungus *Candida albicans* cultured on potato dextrose agar as medium was tested. Ciprofloxacin and Cephalosporin was used as the standard antibacterial and antifungal drug. About 0.5 ml spore suspension of each investigated organisms was added to a sterile petri dishes and left to solidify and the well was made in each plates with the help of a cork-borer (6 mm). The stock solution (10^{-3} mol/L) was prepared by dissolving the compounds in DMSO. The plates were inoculated with microorganisms and filled with the test solution for 24 h for bacteria and 48 h for fungus at 37 °C. The activity was measured in terms of zone of inhibition against bacteria and fungus appearing around the well.

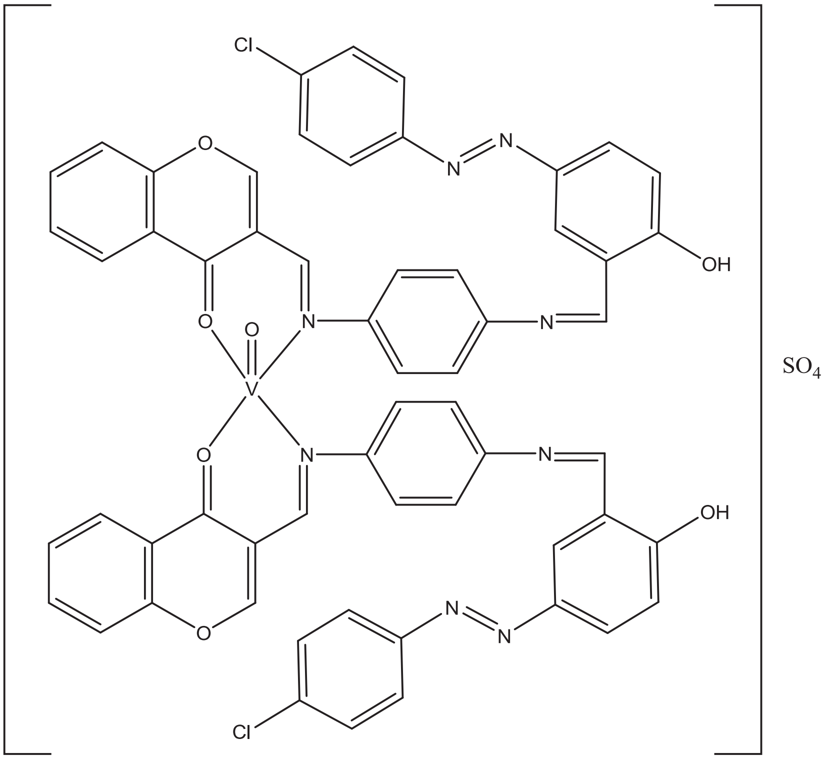

Fig. 3. Proposed Structure of the VO(II) complex.

Results and discussion

The synthesized azo Schiff base ligand CDHBPC and its metal complexes are in good agreement with their formulation as in Table 1. As borne out by the elemental analysis data, the composition of the present complexes was found to be of 1:2 metal:ligand stoichiometry and agree with the proposed formula of ML_2Cl_2 type for Co(II), Ni(II), Cu(II) and Zn(II) complexes (Fig. 2) and $[ML_2]SO_4$ for VO(II) complex (Fig. 3). All the complexes were stable at room temperature and possessed good keeping qualities. They were non-hygroscopic solids and insoluble in ethanol and water but soluble in DMF and DMSO. The lower value of molar conductivity indicates the non-electrolytic behavior [21] of all complexes except oxovanadium complex.

IR spectra

IR spectral data of the ligands and metal complexes are presented in Table 2. The IR spectrum of the free ligand showed characteristic bands at 3056, 1612, 1596, 1520, and 1280 cm^{-1}, assignable to ν(OH), ν(C=O), $\nu(C^a{=}N)$ (azomethine), $\nu(C^b{=}N)$ (arylazomethine) and ν(C–O) (phenolic) stretching modes, respectively [22]. In the complexes, the band due to phenolic –OH vibrations in the 3050–3075 cm^{-1} region, remained unaltered; suggesting the non-involvement of the phenolic proton in the complex formation, and this is further supported by the ν(C–O) vibrations without any change. On complexation, the $\nu(C^a{=}N)$ band is shifted to lower wave numbers (1514–1489 cm^{-1}) with respect to the free ligand, suggesting that the nitrogen of the azomethine group is coordinated to the metal ion. The non involvement of the aryl azomethine in complex formation is observed by the absence of any change in the $\nu(C^b{=}N)$ vibration.

For the cyclic keto group present in the phenyl ring, the frequency of ν(C=O) (1612 cm^{-1}) was shifted to the lower frequency in complexes, suggesting coordination via the C=O oxygen [23]. The sharp band at 1481 cm^{-1} is assigned to the stretching vibration of the diazo group of the ligand and the infrared spectra of the

Table 2
Characteristic IR stretching frequencies (cm^{-1}) of the ligand and its complexes.

Compound	ν (C=O)	N (M–Cl)	ν(N=N)	ν (M–N)	ν(M–O)
[CDHBPC]	1612s	–	1481 s	–	–
$[VOL_2]SO_4$	1605s	–	1480 s	408 m	587 w
$[CoL_2Cl_2]$	1601s	366 m	1482 s	401w	592 w
$[NiL_2Cl_2]$	1600s	368 m	1483 s	418 m	580 m
$[CuL_2Cl_2]$	1608s	379 m	1482 s	418 m	586 m
$[ZnL_2Cl_2]$	1604s	383 m	1480 s	410 w	570 m

s: strong, m: medium, w: weak.

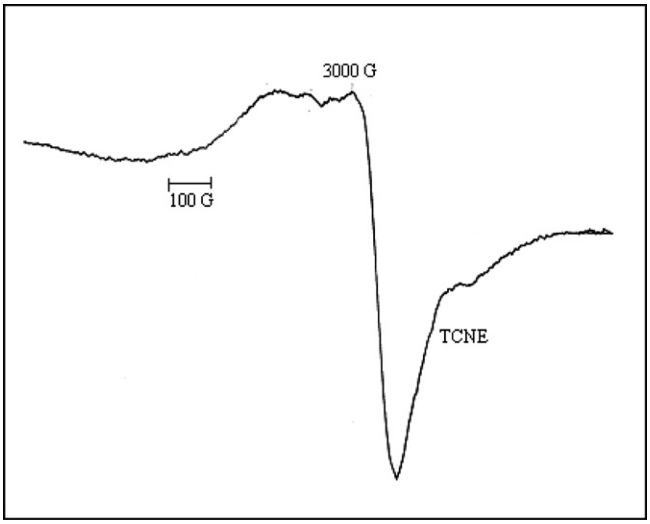

Fig. 4. EPR spectrum of $[C_{58}H_{42}Cl_4N_8O_6Cu]$ at 300 K in DMSO.

Table 3
EPR spectral parameters of VO(II) and copper(II) complexes.

Compound	$g_\parallel$	$g\perp$	g_{iso}	α^2	β^2	$A_\parallel$ (10^{-4} cm^{-1})	$A_\perp$ (10^{-4} cm^{-1})	A_{iso} (10^{-4} cm^{-1})	$g_\parallel/A_\parallel$ (cm)	$K_\parallel$	$K_\perp$	μ (B.M.)
$[VOL_2]SO_4$	1.92	1.96	1.94	1.02	1.09	164	55	91.33	117	1.07	1.03	1.76
$[CuL_2{\cdot}Cl_2]$	2.23	2.10	2.14	0.82	0.36	185	30	81.86	120	0.72	0.44	1.81

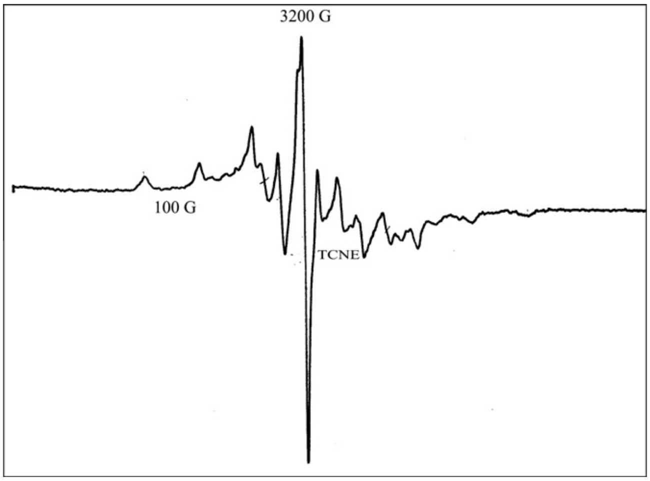

Fig. 5. EPR spectrum of $[C_{58}H_{42}Cl_2N_8O_{11}SV]$ at 300 K in DMSO.

Table 4
Antimicrobial activity of the azo Schiff base ligand and its metal (II) complexes.

Compound	Diameter of the inhibition zone (in mm)[a] against				
	S. aureus	*E. coli*	*S. enterica typhi*	*B. subtilis*	*Candida albicans*
Standard	7	5	5	5	7
CDHBPC	7	7	9	10	11
$[VOL_2]SO_4$	15	10	18	13	9
$[CoL_2Cl_2]$	R	11	9	R	25
$[NiL_2Cl_2]$	18	8	16	R	21
$[CuL_2Cl_2]$	19	23	21	19	13
$[ZnL_2Cl_2]$	20	17	20	17	24

[a] All values are the mean (n = 3) with a standard deviation of <3%; R = Resistant. Standard = (ciprofloxacin and cephalosporin).

complexes did not show any frequency shift of the –N=N– band, which may be explained by non-participation in complex formation [24]. The proof of N and O coordination is demonstrated by bands in the spectra of complexes in the regions 570–592 cm^{-1} and 408–422 cm^{-1} assigned to ν(M–N) and ν(M–O) modes, respectively. The IR spectra of the metal complex show bands in the region 360–383 cm^{-1} assigned to M–Cl bond formation [25]. In the vanadyl complex, a new band appears at 943 cm^{-1} is attributed to V = O frequency [26].

^{1}H NMR spectra

The ^{1}H NMR spectrum of ligand recorded in DMSO has the following signals confirming the structure of the ligand: 10.3 ppm (H, s, OH); 8.3 ppm (H, s, –HC^a=N-azomethine proton); 8.8 ppm (H, s, –HC^b=N-azomethine proton); 6.17–7.90 (m, aromatic protons); The ^{1}H NMR spectrum of zinc(II) complex in DMSO shows the presence of OH proton signal indicating the non involvement of the hydroxyl group in complexation to the metal. However, the resonance signals obtained for azomethine proton (–HC^a=N–) shifted to downfield as compared to the proton NMR of azo Schiff base suggesting the coordination of the azomethine nitrogen to Zn(II) ion.

Mass spectra

The mass spectra of the ligand (CDHBPC) and its complexes are recorded. The molecular ion peak for the Schiff base was observed at 508 m/z. which are in good agreement with the suggested molecular formula indicated from elemental analyses. The molecular ion peak of Cu(II) complex was observed at 1149 m/z, which confirm the stoichiometry of the metal complexes to be $[ML_2Cl_2]$ (Supplementary material, Figs. S1 and S2).

Electronic spectra and magnetic moment

The electronic spectra were recorded in DMSO and the Cu(II) complex shows absorption at 13,698, 15,250 and 24,325 cm^{-1}, which may be assigned to $^2B_{1g} \rightarrow {}^2A_{1g}$ ($d_{x2-y2} \rightarrow d_{z2}$) ($\nu_1$), $^2B_{1g} \rightarrow {}^2B_{2g}$, ($d_{x2-y2} \rightarrow d_{zy}$) ($\nu_2$), $^2B_{1g} \rightarrow {}^2E_g$ ($d_{x2-y2} \rightarrow d_{zy}$, d_{yz}) (ν_3) transitions and the magnetic susceptibility value (1.93 μ_B) confirms the octahedral geometry [26]. The bands at 9407, 16,625 and 18,241 cm^{-1} assigned to $^4T_{1g}(F) \rightarrow {}^4T_{2g}(F)$ [ν_1], $^4T_{1g}(F) \rightarrow {}^4A_{2g}(F)$ [ν_2] and $^4T_{1g}(F) \rightarrow {}^4T_{2g}(P)$ [ν_3] transitions indicates octahedral geometry of the Co(II) complex and the magnetic moment value 4.86 B.M confirms the same [27]. The magnetic moment value 3.26 B.M. for Ni(II) complex as well as the electronic spectrum centered around 9690, 16332 and 23,750 cm^{-1} assigned to $^3A_{2g}(F) \rightarrow {}^3T_{2g}(F)$ [ν_1], $^3A_{2g}(F) \rightarrow {}^3T_{1g}(F)$ [ν_2] and $^3A_{2g}(F) \rightarrow {}^3T_{1g}(P)$ [ν_3] transitions, confirm octahedral geometry around the Ni(II) ion. The octahedral geometry of Co(II) and Ni(II) complexes is further supported by the ratio ν_2/ν_1 which lies around 1.7 and 1.6 [28]. The absorption spectrum of vanadyl complex shows absorption at 12,554, 17,452 and 24,180 cm^{-1} due to $^2B_2 \rightarrow {}^2E_1$, $^2B_2 \rightarrow {}^2B_1$, $^2B_2 \rightarrow {}^2A_1$ transitions, indicating the square pyramidal geometry and the same is further confirmed from its magnetic moment 1.79 B.M. [29]. The Zn(II) complex is diamagnetic and an octahedral geometry for Zn(II) [30].

EPR spectra

The EPR spectrum of the Cu(II) complex was recorded in DMSO at 300 and 77 K (Fig. 4) and the spin Hamiltonian parameters calculated are given in Table 3. The observed spectral parameters show $g_\parallel$ (2.23) > $g_\perp$ (2.10) > g_e (2.0023) which is the characteristic of an octahedral geometry [31] The observed value for the exchange interaction parameter for the Cu(II) complex (G = 2.3) suggests that the significant exchange coupling is present and the misalignment is appreciable. The observed value of α^2 (0.82) of the complex is less than unity, which indicates the covalent character [32]. The magnetic moment of the copper (II) complex is found to be 1.81 B.M. indicative of an unpaired electron. The orbital reduction factors $K_\parallel$ and $K_\perp$ estimated from the expression, $K_\parallel = (g_\parallel - 2.0023)\ \Delta E/8\lambda$, $K_\perp = (g_\perp - 2.0023)\ \Delta E/2\lambda$, $\lambda = -828$ cm^{-1} (spin–orbit coupling constant for the free ion). In case of a pure σ bonding $K_\parallel \cong K_\perp$ 0.77 whereas $K_\parallel < K_\perp$ implies considerable in-plane π-bonding while for out of π bonding $K_\parallel > K_\perp$. For this complex, $K_\parallel > K_\perp$ indicating poor in-plane π-bonding which is also reflected in β^2 values. For oxovanadium complex the calculated

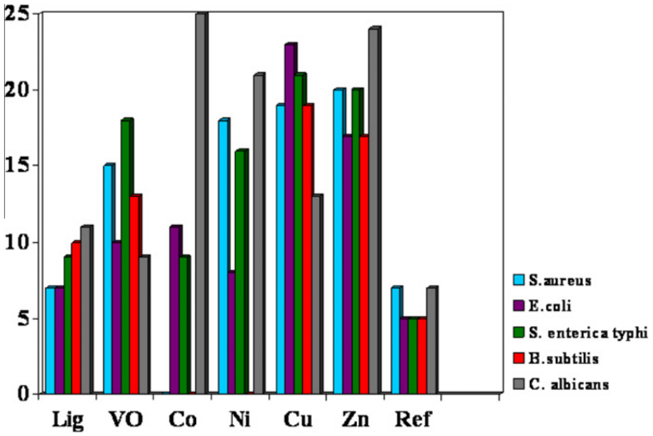

Fig. 6. Biospectrum of azo Schiff base and metal(II) complexes against antibacterial and antifungal strains.

values of $g_{||}$, $g_{\perp}$, g_{av}, for oxovanadium(II) complex are given in Table 3. The g tensor values of this oxovanadium(II) complex can be used to derive the ground state. From the observed values, it is clear that $g_{\perp} > g_{||} > g_e$ (2.0023) suggesting that the complex has square pyramidal geometry [33] with the unpaired electron in the d_{xy} orbital of the metal (Fig. 5).

Antimicrobial study

The ligands and their metal complexes were tested for their inhibitory effects on the growth of bacteria *S. aureus, E. coli, S. enterica typhi, B. subtilis* and fungus *C. albicans,* because microorganisms can achieve resistance to antibiotics through biochemical and morphological modifications [34]. The experimental data presented in Table 4 suggest that the metal complexes are more potent in inhibiting the growth of microorganisms than the ligand against same microorganisms under identical experimental conditions. This would suggest that the chelation could facilitate the ability of a complex to cross a cell membrane and can be explained by Tweedy's chelation theory [35]. The pathogens secreting various enzymes, which are involved in the breakdown of activities, appear to be especially susceptible to inactivation by the ion of complexes. The metal complexes facilitate their diffusion through the lipid layer of spore membrane to the site of action and ultimately killing them by combining with the OH and C=N groups of certain cell enzymes. The Cu(II) and Zn(II) complexes shows greater antibacterial activity towards bacteria and Co(II), Ni(II) and Zn(II) complexes shows greater antifungal activity for *C. albicans* (Fig. 6). The variation in the activity of the metal complexes against different organisms depends on the impermeability of the microorganism cells or on differences in ribosome of microbial cells [36].

Redox behavior

The redox behavior of the copper complex was studied using cyclic voltammetry in order to monitor spectral and structural changes accompanying electron transfer and the results are tabulated in Table 5. The cyclic voltammogram (Supplementary material) of the copper (II) complex in DMSO solvent, recorded at room temperature shows one step reduction cathodic peak for Cu(II) → Cu(0) at E_{pc} = [−0.753 V]. In the anodic side, the direct oxidation of Cu(0) → Cu(II) is observed at E_{pa} = [0.057 V]. The reversibility of the copper(II)/copper (0) couple was checked by varying the scan rates with peak potentials. From Table 5 it is observed that E_{pc} and E_{pa} value changes with the scan rate and ΔE_p values increase with increasing scan rate and is found to be more than 400 mV. The difference in the value of $E_{pa} - E_{pc}$ is ΔE_p which is larger than the value required for a reversible process (59 V) indicating that reduction of Cu(II) at silver electrode is not only diffusion controlled but also by electron transfer kinetics. These observations indicate that the electron transfer process is irreversible [37].

Table 5
Redox potential of the copper(II) complex.

Compound	Scan rate (mV)	E_{pc} (V)	E_{pa} (V)	ΔE_p (V)
[$Cu_2L_2Cl_2$]	100	−0.753	0.057	0.810
	150	−0.726	0.142	0.868
	200	−0.718	0.203	0.921

Nonlinear optical properties of ligand

Nonlinear optics (NLO) properties of organic and inorganic molecules have been the subject of extensive theoretical and experimental investigations during the last two decades. Total first hyperpolarisability (β_{tot}) for Schiff base ligand is studied here and Schiff base shows the better second-harmonic efficiency than urea and KDP. The novel Azo Schiff base show 2.7 and 3.2 times more activity than urea and KDP respectively. Ligand has donor–acceptor property and the electron-withdrawing atom of chlorine can prevent the lone pair electron of nitrogen atom in N=N group to be delocalized and causes a reduction in second-order nonlinearity [38].

Fluorescence study

The fluorescence characteristics of CDHBPC and its complexes were studied at room temperature in DMSO. The emission spectra of ligands excited at 284 nm show an emission peak at 290 nm corresponding to n → π* transition of azomethine group. The Cu(II) complex show strong fluorescence with high-quantum yield (Table 6); excitation at 572 nm gives an emission at 581 nm, assigned to π → π* intraligand fluorescence. Emission intensity of the complexes are higher than that of free ligand and the enhanced fluorescence efficiency of the complexes are attributed to coordination increasing the rigidity, thereby reducing energy loss by thermal vibrational decay [39,40]. Introduction of the substituent on the azo ligand has an interesting effect on the intensity of emission spectra (Fig. 7).

Scanning electron microscopy

The morphology and particle size of the Schiff base Cu(II) complex have been illustrated by the scanning electron micrography (SEM). Fig. 8 depicts the SEM photograph of the synthesized Cu(II) complex. We noted that there is a uniform matrix of the synthesized complex in the pictograph. This leads us to believe that we are dealing with homogeneous phase material. The image of the copper complex depicted in Fig. 8 presents the growth of both

Table 6
Fluorescence characteristic of ligand and its complexes.

Compound	Excitation wavelength (nm)	Fluorescence wavelength (nm)	Quantum yield (φ_f)
CDHBPC	284	290	0.34
[VOL_2]SO_4	799	804	0.78
[CoL_2Cl_2]	841	847	0.73
[NiL_2Cl_2]	845	855	0.81
[CuL_2Cl_2]	572	581	0.36

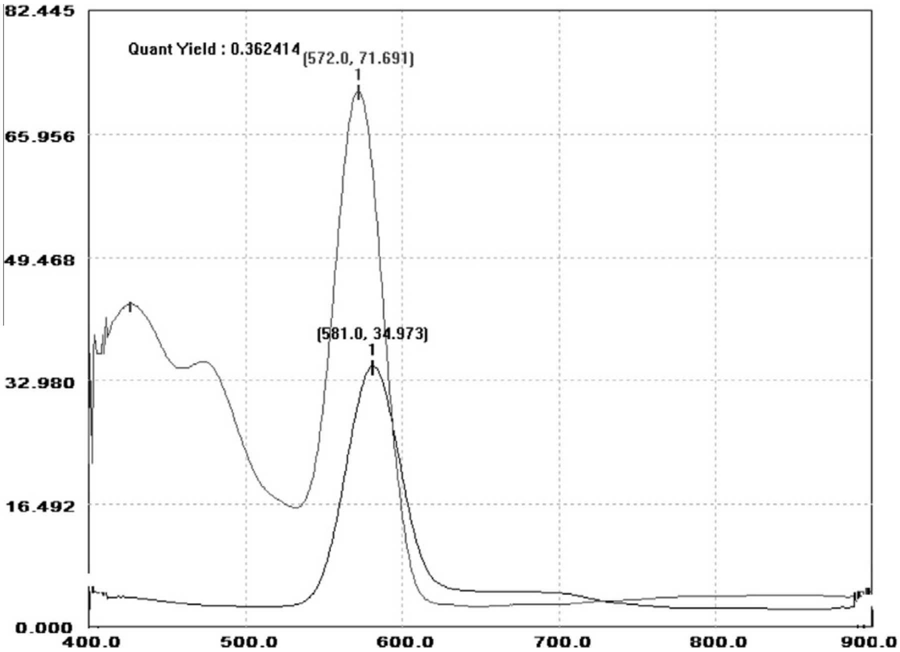

Fig. 7. Emission spectrum of [$C_{58}H_{42}Cl_4N_8O_6Cu$] in DMSO.

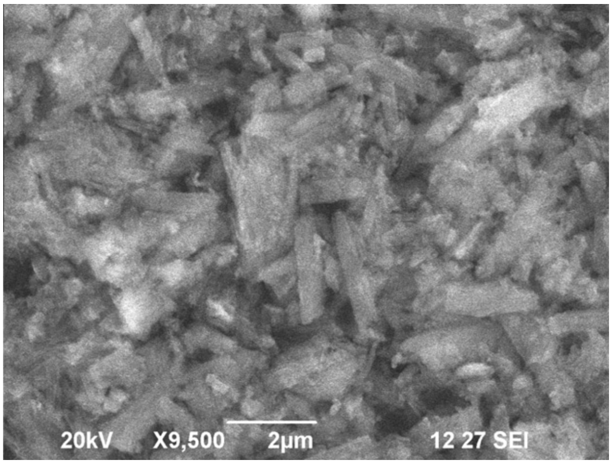

Fig. 8. SEM image of [$C_{58}H_{42}Cl_4N_8O_6Cu$].

vertically and horizontally aligned blocks with irregularity and density and confirms the presences of compounds with the particle size of 2 μm.

Conclusions

The Schiff base complexes of VO(II), Co(II), Ni(II), Cu(II) and Zn(II) derived from 3-(4-5-(4-chlorophenyl)diazenyl)-2-hydroxybenzylideneamino)phenylimino)methyl)-4H-chromen-4-one [CDHBPC] were synthesized and characterized on the basis of analytical and spectral data. The results of this investigation support the suggested octahedral structure of the metal complexes and form a favorable molecular arrangement so that the material show relatively strong solid state NLO properties with the relative SHG efficiency of the material 2.7 and 3.2 times more active than urea and KDP. The Schiff bases and their metal complexes were found to be highly active against the antibacterial and antifungal species. Presence of two azomethine, and a more extended conjugated system shows higher luminescence efficiency of the synthesized compounds. All the compounds are thermally very stable with high melting point and intense color and are attractive from the point of view of studying photoinduced effects in theoretical and experimental areas.

Acknowledgments

Authors thank the Management of The American College, Madurai and one of the authors (CDS) thanks the Defence Research and Development Organization (DRDO) and SAIF, IIT, Bombay and CDRI, (SAIF) Lucknow for providing analytical techniques.

Appendix A. Supplementary data

Supplementary data associated with this article can be found, in the online version, at http://dx.doi.org/10.1016/j.saa.2012.08.022.

References

[1] Y. Shibuya, K. Nabari, M. Kondo, S. Yasue, K. Maeeda, F. Uchida, H. Kawaguchi, Chem. Lett. 37 (2008) 78–79.
[2] B.J. Gangani, P.H. Parsania, Spectrosc. Lett. 40 (2007) 97–112.
[3] G.R. Singh, N.K. Singh, M.P. Girdhar, S. Ishar, Tetrahedron 58 (2002) 2471–2480.
[4] L.Z. Piao, H.R. Park, Y.K. Park, S.K. Lee, J.H. Park, Chem. Pharm. Bull. 50 (2002) 309–311.
[5] G. Athanasellis, G. Melagraki, A. Afantitis, K. Makridima, O. Igglessi Markopoulou, ARKIVOC 10 (2006) 28–34.
[6] L.Z. Piao, H.R. Park, Y.K. Park, S.K. Lee, J.H. Park, M.K. Park, Chem. Pharm. Bull. 50 (2002) 309–311.
[7] R. Kumar, M. Yousuf, ARKIVOC 9 (2006) 239–264.
[8] D. Enders, G. Geibel, S. Osborne, Chem. Eur. J. 6 (2000) 1302–1309.
[9] M.P.S. Ishar, G. Singh, S. Singh, S.K. Satyajit, G. Singh, Bioorg. Med. Chem. Lett. 16 (2006) 1366–1370.
[10] C. Alemán, H.M. Ishiki, J. Org. Chem. 64 (1999) 1768–1769.
[11] R. Polly, P.R. Taylor, J. Phys. Chem. A 103 (1999) 10343–10347.
[12] M. Lacova, A. Puchala, E. Solcanyova, J. Lzc, P. Kois, J. Chovancova, D. Rasata, Molecules 10 (2005) 596–607.
[13] P. Langer, B. Appel, Tetrahedron Lett. 44 (2003) 7921–7923.
[14] A. Sandulache, A.M.S. Silva, J.A.S. Cavaleiro, Tetrahedron 58 (2002) 105–114.
[15] Y.S. Shim, K.C. Kim, D.Y. Chi, K. Lee, H. Cho, Bioorg. Med. Chem. Lett. 13 (2003) 2561–2563.
[16] A. Weissenburg, E.S. Proskaur, J.A. Riddick, E.E. Toope Jr., Organic Solvents in Techniques of organic Chemistry, third ed., Interscience, NewYork, 1995.
[17] K.M. Khan, N. Ambreen, U.R. Mughal, S. Jalil, European, J. Med. Chem. 45 (2010) 4058–4064.
[18] B.S. Furniss, A.J. Hannaferd, V. Rogers (Eds.), Vogel's Textbook of Practical Organic Chemistry, fourth ed., Longman Inc., New York, 1981, p. 716.

[19] S.K. Kurtz, T.T. Perry, J. Appl. Phys. 39 (1968) 3798–3813.

[20] N. Ramana, L. Mitub, A. Sakthivela, M.S.S. Pandia, J. Iran. Chem. Soc. 6 (2009) 738–748.

[21] A. Halve, A. Goyal, Orient. J. Chem. 12 (1996) 87–88.

[22] A.S. Munde, A.N. Jagdale, S.M. Jadhav, T.K. Chondhekar, J. Serb. Chem. Soc. 75 (3) (2010) 349–359.

[23] E. Ispir, M. Kurtoglu, F. Purtas, Transition Met. Chem. 30 (2005) 1042–1047.

[24] M. Tuncel, S. Serin, Transitiom Met. Chem. 31 (2006) 805–812.

[25] M.J. Kharodawala, A.K. Rana, Synth. React. Inorg. Met. Org. Nano-Met. Chem. 33 (2003) 1483–1492.

[26] T. Rosu, E. Pahontu, C. Maxim, R. Georgescu, N. Stanic, Polyhedron 29 (2010) 757–764.

[27] R. Shakru, N.J.P. Subhashini, J. Chem. Pharm. Res. 2 (1) (2010) 38–46.

[28] C.D. Sheela, C. Anitha, P. Tharmaraj, D. Kodimunthiri, J. Coord. Chem. 63 (2010) 884–893.

[29] A. Yadava, H. Yadav, U. Yadav, D. Rao, Turk. J. Chem. 36 (2012) 624–630.

[30] M. Kalanithi, M. Rajarajan, P. Tharmaraj, J. Coord. Chem. 64 (2011) 842–850.

[31] R.N. Patel, A. Singh, K.K. Shukla, D.K. Patel, V.P. Sondhiya, S. Dwivedi, J. Sulfur Chem. 31 (2010) 299–313.

[32] S.K. Hoffmann, J. Goslar, S. Liiewski, K. Basinski, A. Gasowska, L. Lomozik, J. Inorg. Biochem. 111 (2012) 18–24.

[33] R.C. Manurya, S. Rajput, J. Mol. Struct. 794 (2006) 24–34.

[34] E. Ispir, Dyes Pigm. 82 (2009) 13–19.

[35] A.A. Nejo, G.A. Kolawole, M.C. Dumbele, A.R. Opoku, J. Coord. Chem. 63 (2010) 4367–4379.

[36] S.K. Sengupta, O.P. Pandey, B.K. Srivastava, V.K. Sharma, Transition Met. Chem. 23 (1998) 349–352.

[37] S. Chandra, R. Kumar, Spectrochim. Acta Part A 61 (2005) 437–446.

[38] H. Unver, A. Karakas, A. Elmali, T.N. Durlu, J. Mol. Struct. 737 (2005) 131–137.

[39] S.H. Ramadan, R. Ghosh, T.H. Lu, B.K. Ghosh, Polyhedron 24 (2005) 1525–1535.

[40] T. Yu, K. Zhang, Y. Zhao, C. Yang, H. Zhang, L. Qian, D. Fan, W. Dong, L. Chen, Y. Qiu, Inorg. Chim. Acta 361 (2008) 233–240.